Synthesis, Electrochemistry, and Spectroscopic Characterization of Bis-dirhodium Complexes Linked by Axial Ligands

J. L. Bear,*,† B. Han,†,‡ Z. Wu,† E. Van Caemelbecke,†,§ and K. M. Kadish*,†

Department of Chemistry, University of Houston, Houston, Texas 77204−5641, Department of Chemistry, University of Wisconsin−Whitewater, Whitewater, Wisconsin 53190, and Houston Baptist University, 7502 Fondren Road, Houston, Texas 77074-3298

Received November 8, 2000

The synthesis and electrochemical and spectroscopic properties of bis-dirhodium complexes containing ap or dpf bridging ligands, $(ap)_4Rh_2(C{\equiv}C)_2Rh_2(ap)_4$ (**2**) and $(dpf)_4Rh_2(CNC_6H_4NC)Rh_2(dpf)_4$ (**4**), were investigated (where ap and dpf are the 2-anilinopyridinate and *N*,*N*′-diphenylformamidinate ions, respectively). The related "simple" dirhodium species, $(ap)_4Rh_2(C{\equiv}C)_2Si(CH_3)_3$ (**1**) and $(dpf)_4Rh_2(CNC_6H_5)$ (**3**), with the same set of bridging ligands were also synthesized and their properties compared to those of the analogous bis-dirhodium complexes. Compound **1** was obtained by mixing $(ap)_4Rh_2Cl$ and $Li(C{\equiv}C)_2Si(CH_3)_3$ in refluxing THF for 16 h under vacuum while compound **2** was prepared by a reaction between $(ap)_4Rh_2(C{\equiv}C)_2Li$ and $(ap)_4Rh_2Cl$ under similar conditions. The reaction between $(CF_3COO)_4Rh_2$ and molten Hdpf under vacuum for 24 h leads to the generation of compound **3** with a yield of 65%. The red-orange compound **4** was obtained upon addition of 0.5 equiv of CNC_6H_4NC at room temperature to a CH_2Cl_2 solution containing $(dpf)_4Rh_2$ which was synthesized according to a method described previously in the literature. Compound **1** crystallizes in the triclinic space group $P\bar{1}$, with $a = 10.164(3)$ Å, $b = 13.881(3)$ Å, $c = 18.805(4)$ Å, $\alpha = 73.55(2)°$, $\beta = 77.89(2)°$, $\gamma = 84.85(2)°$, and $Z = 2$. Crystals of **2** were not good enough to collect adequate data for X-ray analysis, but the identity of this compound was confirmed, along with its $P\bar{1}$ space group. Crystals of **3** and **4** belong to the monoclinic, $P2_1/c$ space group and the triclinic, $P\bar{1}$ space group, respectively, with $a = 13.5254(5)$ Å, $b = 13.7387(4)$ Å, $c = 27.2011(12)$ Å, $\beta = 102.637(2)°$, and $Z = 4$ for **3** and $a = 13.866(8)$ Å, $b = 14.756(7)$ Å, $c = 15.008(6)$ Å, $\alpha = 79.91(3)°$, $\beta = 87.72(4)°$, $\gamma = 89.19(4)°$, and $Z = 1$ for **4**. Compound **1** exhibits a single reversible oxidation at $E_{1/2} = 0.66$ V and a single reversible reduction at $E_{1/2} = -0.44$ V vs SCE in THF, 0.2 M TBAP. Both processes involve a one-electron transfer. Compound **2** undergoes a reversible oxidation at $E_{1/2} = 0.60$ V and two separate one-electron-transfer reductions at $E_{1/2} = -0.52$ and -0.65 V in THF, 0.2 M TBAP. The oxidation involves two overlapped one-electron-transfer processes. Compounds **3** and **4** undergo two reversible oxidations in CH_2Cl_2, 0.1 M TBAP located at $E_{1/2} = 0.23$ and 1.22 V (**3**) or 0.22 and 1.20 V (**4**). Each redox reaction of **3** involves a one-electron-transfer step while each redox reaction of **4** involves two overlapping one-electron transfers. Compound **2** shows interaction between the two dirhodium cores upon reduction, while **4** gives no evidence of electronic interaction between the two dirhodium units during either reduction or oxidation. An ESR signal with axial symmetry was obtained for the neutral compounds **1** and **2**, and a similar spectrum was obtained for the singly oxidized products of compounds **3** and **4**, thus suggesting the electronic configuration of $(\sigma)^2(\pi)^4(\delta)^2(\pi^*)^4(\delta^*)^1$ for the neutral compounds **1** and **2** as well as for the oxidized compounds **3** and **4**. The four compounds were also characterized by FTIR and UV−visible spectroscopy as well as by mass spectrometry.

Introduction

The first isolation of a tetrakis(carboxylato) compound of the type $Rh_2(O_2CR)_4$ was described in 1960,[1] and this was followed over the years by the synthesis of a large number of other dirhodium complexes with tetracarboxylate type structures,[2−25] many of which were also characterized as to their structural, electrochemical, and/or spectroscopic properties. The tetra-

† University of Houston.
‡ University of Wisconsin−Whitewater.
§ Houston Baptist University.

(1) Chernyaev, I. I.; Shenderetskaya, E. V.; Karyaguba, A. A. *Russ. J. Inorg. Chem.* **1960**, *5*, 559.
(2) Cotton, F. A.; Dikarev, E. V.; Stiriba, S.-E. *Inorg. Chem.* **1999**, *38*, 4877.
(3) Cotton, F. A.; Dikarev, E. V.; Petrukhina, M. A.; Stiriba, S.-E. *Organometallics* **2000**, *19*, 1402.
(4) Cotton, F. A.; Dikarev, E. V.; Stiriba, S.-E. *Organometallics* **1999**, *18*, 2724.
(5) Tocher, D. A.; Tocher, J. H. *Inorg. Chim. Acta* **1985**, *104*, L15.
(6) Bear, J. L.; Liu, L. M.; Kadish, K. M. *Inorg. Chem.* **1987**, *26*, 2929.
(7) Bear, J. L.; Yao, C.-L.; Liu, L.-M.; Capdevielle, F. J.; Korp, J. D.; Albright, T. A.; Kang, S.-K.; Kadish, K. M. *Inorg. Chem.* **1989**, *28*, 1254.
(8) Yao, C.-L.; Park, K. H.; Khokkar, A. R.; Jun, M.-J.; Bear, J. L. *Inorg. Chem.* **1990**, *29*, 4033.
(9) Cotton, F. A.; Felthouse, T. R. *Inorg. Chem.* **1980**, *19*, 2347.
(10) Cotton, F. A.; Felthouse, T. R. *Inorg. Chem.* **1981**, *20*, 584.
(11) Zhu, T. P.; Ahsan, M. Q.; Malinski, T.; Kadish, K. M.; Bear, J. L. *Inorg. Chem.* **1984**, *23*, 2.
(12) Norman, J. G.; Kolari, H. *J. Am. Chem. Soc.* **1978**, *100*, 791.
(13) Schiavo, S. L.; Bruno, G.; Zanello, P.; Laschi, F.; Piraino, P. *Inorg. Chem.* **1997**, *36*, 1004.
(14) Martin, D. S.; Webb, T. R.; Robbins, G. A.; Fanwick, P. E. *Inorg. Chem.* **1979**, *18*, 475.
(15) Pruchnik, F. P.; Robert, F.; Jeannin, Y.; Jeannin, S. *Inorg. Chem.* **1996**, *35*, 4261.
(16) Bear, J. L.; Yao, C.-L.; Lifsey, R. S.; Korp, J. D.; Kadish, K. M. *Inorg. Chem.* **1991**, *30*, 336.

10.1021/ic001245f CCC: $20.00
Published on Web 04/03/2001

Chart 1

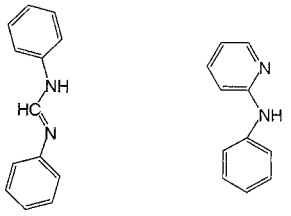

Hdpf Hap

Chart 2

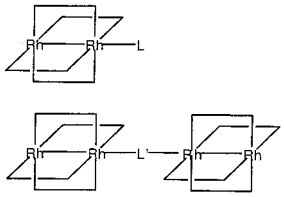

ap: L = $(C{\equiv}C)_2Si(CH_3)_3$ and L' = $(C{\equiv}C)_2^{2-}$

bridged dirhodium complexes investigated to date can be classified as "monomeric" [1,5−25] or, in some cases, as "polymeric" [2−4] species, but little is known as to how the electronic and spectroscopic properties of these compounds might be altered when the two dirhodium complexes are axially linked to each other via a rigid spacer. This point is examined in the present paper which reports the synthesis, spectroscopic properties, and electrochemical characterization of two bis-dirhodium complexes represented as $(ap)_4Rh_2(C{\equiv}C)_2Rh_2(ap)_4$ (**2**) and $(dpf)_4Rh_2(CNC_6H_4NC)Rh_2(dpf)_4$ (**4**) where ap and dpf are the 2-anilinopyridinate and *N*,*N*′-diphenylformamidinate ions, respectively. The dpf ligand is symmetrical, and complexes with this bridging ligand exist in a single isomeric form, while the ap ligand is unsymmetrical (see Chart 1), and complexes with this bridging ligand can in principle exist in four different isomeric forms.[26] However, all of the dirhodium or bis-dirhodium complexes with ap bridging ligands examined in the present paper exist in the (4,0) isomeric conformation.[7,8,26]

For comparison with the two examined bis-dirhodium species, two related dirhodium complexes with the same four ap or dpf anionic bridging ligands, $(ap)_4Rh_2(C{\equiv}C)_2Si(CH_3)_3$ (**1**) and $(dpf)_4Rh_2(CNC_6H_5)$ (**3**), were synthesized and examined as to their structural, electrochemical, and spectroscopic properties. The compounds which are described in this paper are shown schematically in Charts 2 and 3.

The combined electrochemical, spectroscopic, and structural behavior of the above compounds should provide data on the electronic interaction between the two dirhodium units in their neutral, electroreduced, and/or electrooxidized forms.

Chart 3

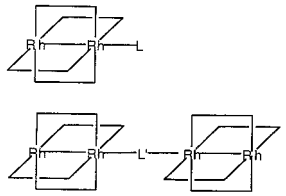

dpf: L = CNC_6H_5 and L' = CNC_6H_4NC

Experimental Section

Chemicals. 2-Anilinopyridine (Hap) and *N*,*N*′-diphenylformamidine (Hdpf) were purchased from Aldrich Chemical Co. and recrystallized from dichloromethane and hexane. The rhodium(II) acetate dimer, $(O_2CCH_3)_4Rh_2$, purchased from Strem Chemical Co. as well as 1,4-phenylene diisocyanide (CNC_6H_4NC) and butyllithium (BuLi), purchased from Aldrich Chemical Co., were used without purification. 1,4-Bis(trimethylsilyl)-1,3-butadiyne, $((CH_3)_3Si(C{\equiv}C)_2Si(CH_3)_3)$ obtained from Farchan Laboratories, Inc., was used as received. The supporting electrolyte, tetra-*n*-butylammonium perchlorate (TBAP) (Fluka Chemical Co.), was twice recrystallized from absolute ethanol. It was dried in a vacuum oven at 40 °C for 1 week and stored in a desiccator at room temperature prior to use. Dichloromethane (CH_2Cl_2) from Mallinckrodt, Inc., was refluxed over P_2O_5 under Ar for 30 min prior to distillation. Tetrahydrofuran (THF), also purchased from Mallinckrodt Inc., was first distilled over CaH_2 followed by a distillation over sodium/benzophenone under Ar. Ar (4.8 Grade, Trigas, Co.) was passed through an activated copper powder column and a molecular sieve column to remove any traces of oxygen and water prior to use.

Instrumentation. Cyclic voltammetry and normal pulse and differential pulse voltammetric measurements were carried out on an IBM EC 225 voltammetric analyzer using a conventional three-electrode system which consisted of a platinum button working electrode (1.0 mm diameter), a platinum wire counter electrode, and a homemade saturated calomel reference electrode (SCE) which was separated from the bulk solution by a platinum-tipped glass frit. Argon gas was used to remove any oxygen from the solution and to maintain an inert atmosphere above the solution during the electrochemical experiments. All potentials are reported versus the SCE. Controlled-potential bulk electrolyses were performed with a homemade "H" type cell into which were placed the working and a counter platinum gauze electrodes that were separated by a fine fritted disk. A platinum-tipped bridge was used to separate the reference electrode from the bulk solution.

IR spectral measurements were made on a Nicolet 740 infrared spectrometer. The samples were run as CsI pellets. Raman spectra were recorded by using a SPEX 1403 double-monochromator equipped with a Hamumatsu R928 photomultiplier tube. Excitation wavelengths were provided by a coherent K-2 Kr^+ ion laser (406.7, 520.8, 530.9, and 647.1 nm). Spectra were obtained with rotating KCl pellets at room temperature or were recorded at 77 K while scattered light was collected with a 135° backscattering geometry. UV−visible spectra were obtained with a Perkin-Elmer 330 UV−vis spectrophotometer, and samples of electrogenerated products were transferred under argon via a cannula from the electrolysis cell to a quartz cuvette. ESR measurements were recorded at 77 K with a modified Varian E-4 ESR spectrometer that was interfaced with a Tracor Northern TN-1710 signal averager. Each spectrum was obtained by multiple scans to achieve a satisfactory signal-to-noise ratio. The magnetic field was calibrated with a Varian E-500 gaussmeter while the microwave frequency was monitored by a Hewlett-Packard HP5342A microwave frequency counter. All *g* values are referenced versus diphenylpicrylhydrazyl (DPPH) which has a *g* value of 2.0036.[27] Mass spectra were obtained on a VG analytical model

(17) Das, K.; Kadish, K. M.; Bear, J. L. *Inorg. Chem.* **1978**, *17*, 930.
(18) Piraino, P.; Bruno, G.; Schiavo, S. L.; Laschi, F.; Zanello, P. *Inorg. Chem.* **1987**, *26*, 2205.
(19) Kadish, K. M.; Lancon, D.; Dennis, A. M.; Bear, J. L. *Inorg. Chem.* **1982**, *21*, 2987.
(20) Lifsey, R. S.; Chavan, M. Y.; Chan, L. K.; Ahsan, M. Q.; Kadish, K. M.; Bear, J. L. *Inorg. Chem.* **1987**, *26*, 822.
(21) Asara, J. M.; Hess, J. S.; Lozada, E.; Dunbar, K. R.; Allison, John. *J. Am. Chem. Soc.* **2000**, *122*, 8.
(22) Catalan, K. V.; Hess, J. S.; Maloney, M. M.; Mindiola, D. J.; Ward, D. L.; Dunbar, K. R. *Inorg. Chem.* **1999**, *38*, 3904.
(23) Lichtenberg, D. L.; Pollard, J. R.; Lynn, M. A.; Cotton, F. A.; Feng, X. *J. Am. Chem. Soc.* **2000**, *122*, 3182.
(24) Chakravarty, A. R.; Cotton, F. A.; Tocher, D. A.; Tocher, J. H. *Inorg. Chim. Acta* **1985**, *101*, 185.
(25) Bursten, B. E.; Cotton, F. A. *Inorg. Chem.* **1981**, *20*, 3042.
(26) Bear, J. L.; Li, Y. L.; Han, B. C.; Caemelbecke, E. V.; Kadish, K. M. *Inorg. Chem.* **1997**, *36*, 5449.
(27) Drago, R. S. *Physical Methods in Chemistry*; W. B. Saunders: Philadephia, PA, 1977; p 305.

Table 1. X-ray Data Collection and Processing Parameters

	$(ap)_4Rh_2(C{\equiv}C)_2Si(CH_3)_3$ (**1**)	$(dpf)_4Rh_2(CNC_6H_5)$ (**3**)	$(dpf)_4Rh_2(CNC_6H_4NC)Rh_2(dpf)_4$ (**4**)
space group	$P\bar{1}$	$P2_1/c$	$P\bar{1}$
cell constants			
a, Å	10.164(3)	13.5254(5)	13.866(8)
b, Å	13.881(3)	13.7387(4)	14.756(7)
c, Å	18.805(4)	27.2011(12)	15.008(6)
α, deg	73.55(2)	90	79.91(3)
β, deg	77.89(2)	102.673(2)	87.72(4)
γ, deg	84.85(2)	90	89.19(4)
V, Å^3	2487	4931	3021
mol formula	$C_{51}H_{45}N_8SiRh_2{\cdot}^1/_2C_6H_{14}$	$C_{59}H_{49}N_9Rh_2$	$C_{112}H_{92}N_{18}Rh_4{\cdot}6CH_2Cl_2$
MW	1047.05	1089.89	2611.44
Z	2	4	1
ρ, g/cm^3	1.40	1.468	1.44
μ, cm^{-1}	7.19	7.19	8.48
λ (Mo Kα), Å	0.71073	0.71073	0.71073
$R(F_o)^a$	0.037	0.042	0.044
$R_w(F_o)^b$	0.041	0.1095[c]	0.040
total data collected	6465	21505	5631
indep data $I > 3\sigma(I)$	5169	10881	4383
temp (K)	293	133	293

[a] $R = \sum||F_o| - |F_c||/\sum|F_o|$. [b] $R_w = [\sum w(|F_o| - |F_c|)^2/\sum w|F_o|^2]^{1/2}$. [c] Value given is wR2 $= [\sum w(F_o^2 - F_c^2)^2/\sum wF_o^4]^{1/2}$; $w = 1/[\sigma^2(F_o^2) + (0.0259P)^2 + 10.0013P]$ where $P = [F_o^2 + 2F_c^2]/3$.

70-SEQ mass spectrometer using fast atom bombardment (FAB) with *m*-nitrobenzyl alcohol (NBA) as the matrix.

Synthesis of $(ap)_4Rh_2Cl$. $(ap)_4Rh_2Cl$ was prepared by a method which has been modified from a method previously described in the literature.[6−8] $(O_2CCF_3)_4Rh_2$ and Hap were mixed in a 1:8 molar ratio in toluene and refluxed at 109 °C for 20 h. The solvent was removed using a rotary evaporator. The remaining residue was dissolved in CH_2Cl_2 containing 30% CCl_4 (v/v) and left to stand for 2−3 h in sunlight to generate $(ap)_4Rh_2Cl$. The product was purified on a silica gel column and eluted with a 5:95 (v/v) ethanol/dichloromethane mixture. A red band was collected, and, after evaporation of the eluent, $(ap)_4Rh_2Cl$ was obtained in a 65% yield.

Synthesis of $(ap)_4Rh_2(C{\equiv}C)_2Si(CH_3)_3$, 1. This compound was obtained by mixing 30 mL of a THF solution of $(ap)_4Rh_2Cl$ (0.11 mmol) and 10 mL of $Li(C{\equiv}C)_2Si(CH_3)_3$ (0.22 mmol) under Ar, which was synthesized according to a procedure described in the literature.[28] The mixture was then refluxed for 16 h, during which time the color of the solution changed from red to red-brown. The solvent was removed and the product twice purified on a silica gel column using CH_2Cl_2 as eluent. The complex was then recrystallized from CH_2Cl_2/hexane and obtained with a yield of 92%. Mass spectral data [*m*/*e* (fragment)]: 1003, $[(ap)_4Rh_2(C{\equiv}C)_2Si(CH_3)_3]^+$; 931, $[(ap)_4Rh_2C{\equiv}CC{\equiv}CH]^+$; 883, $[(ap)_4Rh_2]^+$. UV−visible data in THF [*λ* (nm, *ϵ*)]: 450 (3.4 × 10^3); 520 (2.9 × 10^3); 830 (7.3 × 10^3); 1600 (3.0 × 10^3).

Synthesis of $(ap)_4Rh_2(C{\equiv}C)_2Rh_2(ap)_4$, 2. $(ap)_4Rh_2(C{\equiv}C)_2Li$ was first obtained by reacting $(ap)_4Rh_2(C{\equiv}C)_2Si(CH_3)_3$ with BuLi in a 1:1.5 molar ratio in THF at room temperature under Ar. Then 15 mL of a THF solution of $(ap)_4Rh_2(C{\equiv}C)_2Li$ (0.55 mmol) was transferred under Ar to 25 mL of a THF solution of $(ap)_4Rh_2Cl$ (0.71 mmol). The mixture was refluxed for 20 h, after which the solvent was removed using a rotary evaporator. Dichloromethane was then added to the solid mixture to dissolve most of the unreacted starting materials, and the remaining solid was collected by filtration. The product was further purified on a silica gel column using THF as the eluent. A green band was collected and the product obtained in a yield of 35%. Mass spectral data [*m*/*e* (fragment)]: 1813, $[(ap)_4Rh_2(C{\equiv}C)_2Rh_2(ap)_4]^+$; 931, $[(ap)_4Rh_2C{\equiv}CC{\equiv}CH]^+$; 883, $[(ap)_4Rh_2]^+$. Anal. Calcd for $C_{92}H_{74}N_{16}Rh_4$: C, 60.93; H, 3.97; N, 12.36; Rh, 22.73. Found: C, 60.68; H, 4.15; N, 12.30; Rh, 22.53. UV−visible data in THF [*λ* (nm, *ϵ*)]: 455 (5.2 × 10^3); 620 (4.5 × 10^3); 915 (7.1 × 10^3); 1600 (3.2 × 10^3).

Synthesis of $(dpf)_4Rh_2(CNC_6H_5)$, 3. The reaction between $(O_2CCF_3)_4Rh_2$ (0.1 g, 0.2 mmol) and molten Hdpf (6.0 g, 31 mmol) under a vacuum for 24 h gives $(dpf)_4Rh_2(CNC_6H_5)$ and is associated with a color change from yellow-green to red.[29] Excess Hdpf ligand was removed by sublimation under vacuum at 120 °C. The residue was then purified on an alumina column using CH_2Cl_2 as the eluent, and the title compound was obtained with a yield of 65%. Crystals of **3** were obtained by slow diffusion of hexane into a CH_2Cl_2/benzene (99:1, v:v) solution of $(dpf)_4Rh_2(CNC_6H_5)$. Mass spectral data [(*m*/*e*, fragment)]: 1089, $[(dpf)_4Rh_2(CNC_6H_5)]^+$; 987 $[Rh_2(dpf)_4]^+$. Anal. Calcd for $C_{59}H_{49}N_9Rh_2{\cdot}CH_2Cl_2$: C, 61.32; H, 4.36; N, 10.07. Found: C, 60.96; H, 4.57; N, 10.03.

Synthesis of $(dpf)_4Rh_2(CNC_6H_4NC)Rh_2(dpf)_4$, 4. The compound was synthesized by reacting $(dpf)_4Rh_2$[16] with 0.5 equiv of 1,4-phenylene diisocyanide (CNC_6H_4NC). The solution of CNC_6H_4NC in CH_2Cl_2 was added dropwise at room temperature into a dilute CH_2Cl_2 solution of $(dpf)_4Rh_2$. Upon addition of CNC_6H_4NC, the color of the solution changed from yellow-green to red-orange. The solvent was then evaporated under vacuum, and the product was purified on a silica gel column using CH_2Cl_2 as the eluent. The title compound was recovered in an 80% yield. Crystals of **4** were obtained by a slow evaporation of a CH_2Cl_2 solution of the compound. Mass spectral data (*m*/*e*, fragment): 2102, $[(dpf)_4Rh_2CNC_6H_4NCRh_2(dpf)_4]^+$; 987 $[Rh_2(dpf)_4]^+$. Anal. Calcd for $C_{112}H_{92}N_{18}Rh_4$: C, 63.75; H, 4.71; N, 11.05. Found: C, 63.94; H, 4.38; N, 11.99. UV−visible data in THF [*λ* (nm, *ϵ*)]: 530 nm (4.2 × 10^3). IR (CsI pellet): $\nu_{CN} = 2125$ cm^{-1}.

X-ray Crystallography. Single-crystal X-ray diffraction studies of compounds **1**, **2**, and **4** were performed at the University of Houston using a Nicolet R3m/V automatic diffractometer while crystals of compound **3** were analyzed at the University of Wisconsin−Madison using a Bruker SMART CCD area detector mounted on a Bruker P4 goniometer. The radiation used was Mo Kα monochromatized by a highly ordered graphite crystal. Samples of **1**, **2,** and **4** were coated with a thin layer of epoxy in order to retard solvent loss. Nicolet's SHELXTL PLUS (1987) series of crystallographic programs were used to solve and refine compounds **1**, **2**, and **4**, while SHELX97 was used for compound **3**. Final cell constants, as well as other information pertinent to data collection and refinement, are listed in Table 1.

$(ap)_4Rh_2(C{\equiv}C)_2Si(CH_3)_3$ (1). A dark burgundy colored thick column having approximate dimensions 0.70 × 0.22 × 0.14 mm was used for X-ray analysis. Intensities were measured using the omega techniques,

(28) Salaun, J.; Ollivier, J. *Nouv. J. Chim.* **1981**, *5*, 587.

(29) The CNC_6H_5 axial ligand comes from a decomposition of Hdpf during the 24 h of reaction time, and the same final compound was reproducibly formed for different batches of purified or unpurified Hdpf. The decomposition of Hdpf does not appear to occur at shorter reaction times and lower temperatures. Thus a reaction between Hdpf and $(O_2CCH_3)_4Rh_2$ gives $(dpf)_4Rh_2$ in high yield[16] when the reaction mixture is heated at 130 °C and stirred for 10 h under vacuum.

and the structure was solved by interpretation of the Patterson map. The axial ligand did not refine well at all and was eventually determined to be disordered over three major positions. Each of these separate orientations was given a population of 33% and refined as a rigid body. Additionally, a molecule of hexane solvent was located about an inversion center. The solvent is probably quite disordered, and only the major position refined, with populations of only 40% for each of the three independent atoms involved. It is assumed that the solvent site is fully occupied, and all values in Table 1 are based on this assumption.

$(ap)_4Rh_2(C{\equiv}C)_2Rh_2(ap)_4$ (2). Several crystals of the compound were examined, and all showed very weak scattering regardless of the sample size. Eventually, one specimen was found which gave enough data to confirm the identity of the compound. The structure of the bis-dirhodium species was found to be a complex mixture of optical isomers, with both left-handed and right-handed orientations of the dimer metal equatorial planes occurring on each side of the inversion center. The compound is apparently a randomly dispersed mixture of +/+, −/−, +/−, and −/+ optical isomers, in equal ratios. Unfortunately, the disorder was so large and the amount of data so little that the least squares refinement had to be abandoned. There were also molecules of disordered solvent present in the cell, making the analysis of the structure even more difficult. Despite the problems and the absence of accurate values for bond lengths and bond angles, the X-ray data strongly suggest that the molecular structure of the compound consists of a pair of linked Rh_2 units bridged by 1,3-butadiyne.

$(dpf)_4Rh_2(CNC_6H_5)$ (3). A dark red plate-shaped crystal of dimensions 0.35 × 0.35 × 0.05 mm was selected for structural analysis. The sample was cooled to 133 K. The intensity data, which nominally covered one-half hemisphere of reciprocal space, were measured as a series of ϕ oscillation frames each of 0.30° for 30 s/frame. Cell parameters were determined from a nonlinear least-squares fit of 6194 peaks in the range $3.0° < \theta < 25.0°$. The first 50 frames were repeated at the end of data collection, showing a maximum variation of 0.01%. A total of 21505 data were measured in the range $1.53° < \theta < 28.43°$. The data were corrected for absorption by the semiempirical method, giving minimum and maximum transmission factors of 0.710 and 0.862. The data were merged to form a set of 10881 independent data with $R(\text{int}) = 0.0300$. The monoclinic space group $P2_1/c$ was determined by systematic absences. The structure was solved by direct methods and refined by full-matrix least-squares on F^2.

$(dpf)_4Rh_2(CNC_6H_4NC)Rh_2(dpf)_4$ (4). A dark carmine colored block having approximate dimensions 0.80 × 0.45 × 0.40 mm was cut from a fused conglomerate and used in the analysis. The data showed a 30% decay over the course of the experiment, and a linear normalization factor as a function of X-ray exposure time was applied to account for this. The structure was solved by interpretation of the Patterson map. The central phenyl ring was found to be disordered, having two distinct orientations about the inversion center. The two orientations are 61° apart and present in equal amounts (50% occupancy for each). Additionally, three independent solvent sites were found in the asymmetric unit, each heavily disordered with at least two major molecular orientations. The disorder problem was partially solved by refining ideal rigid body models at each major position, and all values in Table 1 are based on a 100% occupancy at each solvent site.

Results and Discussion

Synthesis and Spectroscopic Characterization. The bis-dirhodium complex $(ap)_4Rh_2(C{\equiv}C)_2Rh_2(ap)_4$ (**2**) was obtained in 35% yield via a reaction between $(ap)_4Rh_2(C{\equiv}C)_2Li$ and $(ap)_4Rh_2Cl$ under an argon atmosphere as described in eq 1.

$$(ap)_4Rh_2(C{\equiv}C)_2Li + (ap)_4Rh_2Cl \rightarrow (ap)_4Rh_2(C{\equiv}C)_2Rh_2(ap)_4 + LiCl \quad (1)$$

Assignment of the product as $(ap)_4Rh_2(C{\equiv}C)_2Rh_2(ap)_4$ was made on the basis of spectroscopic data (see Experimental Section) and preliminary structural data (see following pages) as well as on its mass spectrum, which exhibited the parent molecular ion peak at $m/e = 1813$. Both Raman and IR spectra are also consistent with its molecular structure. A band is seen at 2123 cm^{-1} in the Raman spectrum of $(ap)_4Rh_2(C{\equiv}C)_2Rh_2(ap)_4$, and this feature is assigned to the C≡C vibration of the compound.

Table 2. Selected Bond Lengths (Å) of $(ap)_4Rh_2(C{\equiv}C)_2Si(CH_3)_3$ (**1**) $(dpf)_4Rh_2(CNC_6H_5)$ (**3**), and $(dpf)_4Rh_2(CNC_6H_4NC)Rh_2(dpf)_4$ (**4**)

$(ap)_4Rh_2(C{\equiv}C)_2Si(CH_3)_3$ (**1**)			
Rh(1)−Rh(2)	2.443(1)	Rh(1)−C(45)	2.028(7)
Rh(1)−N(1)	2.057(5)	Rh(1)−N(3)	2.044(4)
Rh(1)−N(5)	2.056(4)	Rh(1)−N(7)	2.054(4)
Rh(2)−N(2)	2.005(4)	Rh(2)−N(4)	2.007(4)
Rh(2)−N(6)	2.005(4)	Rh(2)−N(8)	2.002(5)
C(45)−C(46)	1.188(11)		
$(dpf)_4Rh_2(CNC_6H_5)$ (**3**)			
Rh(1)−Rh(2)	2.4798(4)	Rh(1)−C(53)	1.991(4)
Rh(1)−N(1)	2.066(3)	Rh(1)−N(3)	2.064(3)
Rh(1)−N(5)	2.058(3)	Rh(1)−N(7)	2.054(3)
Rh(2)−N(2)	2.047(3)	Rh(2)−N(4)	2.050(3)
Rh(2)−N(6)	2.049(3)	Rh(2)−N(8)	2.059(3)
C(53)−N(9)	1.149(4)	C(54)−N(9)	1.398(5)
$(dpf)_4Rh_2(CNC_6H_4NC)Rh_2(dpf)_4$ (**4**)			
Rh(1)−Rh(2)	2.496(1)	Rh(1)−C(53)	1.988(9)
Rh(1)−N(1)	2.054(7)	Rh(1)−N(3)	2.063(6)
Rh(1)−N(5)	2.055(8)	Rh(1)−N(7)	2.037(6)
Rh(2)−N(2)	2.030(7)	Rh(2)−N(4)	2.038(6)
Rh(2)−N(6)	2.051(7)	Rh(2)−N(8)	2.046(6)
C(53)−N(9)	1.142(12)	C(54)−N(9)	1.406(14)

The bis-dirhodium complex $(dpf)_4Rh_2(CNC_6H_4NC)Rh_2(dpf)_4$ (**4**) was obtained in 80% yield by a reaction between $(dpf)_4Rh_2$ and CNC_6H_4NC as shown by eq 2. In this reaction,

$$2(dpf)_4Rh_2 + CNC_6H_4NC \rightarrow (dpf)_4Rh_2(CNC_6H_4NC)Rh_2(dpf)_4 \quad (2)$$

CNC_6H_4NC was added slowly to a solution of $(dpf)_4Rh_2$ until a maximum molar ratio of 2:1 [$(dpf)_4Rh_2$:CNC_6H_4NC] was obtained. This ratio was used to avoid a possible polymerization of the dirhodium complex which occurs when an excess of CNC_6H_4NC is added to solution.[30]

Formation of $(dpf)_4Rh_2(CNC_6H_4NC)Rh_2(dpf)_4$ (**4**) was confirmed by the spectroscopic and analytical data (see Experimental Section) and by its mass spectrum, which exhibited the protonated molecular ion peak at $m/e = 2102$. The infrared spectrum of the compound is characterized by a band at 2125 cm^{-1} assigned to the vibration of the CN bond in the CNC_6H_4NC bridging ligand. This value is similar to the 2131 cm^{-1} found for the CN vibration in free CNC_6H_4NC, thus indicating that the π back-donation from the dirhodium centers to CNC_6H_4NC is weak in compound **4**. This result is also consistent with the fact that the CN bond distances in this compound are essentially the same as the CN bond distances in the free axial ligand, CNC_6H_4NC.

Molecular Structures. Selected bond lengths and bond angles for compounds **1**, **3**, and **4** are summarized in Tables 2 and 3, and X-ray crystal structures of the four compounds are given in Figures 1 and 2. As mentioned above, $(ap)_4Rh_2(C{\equiv}C)_2Rh_2(ap)_4$ (**2**) shows a massive disorder and it was not possible to determine the exact bond lengths and bond angles in this compound. A comparison of structural data between $(ap)_4Rh_2(C{\equiv}C)_2Si(CH_3)_3$ (**1**) and the analogous compound, $(ap)_4Rh_2C{\equiv}CH$,[8] shows that little difference exists between the two

(30) Addition of excess CNC_6H_4NC into a solution of $(dpf)_4Rh_2$ gives an insoluble red-orange compound believed to be a polymer in which the dirhodium units are linked to each other via the CNC_6H_4NC group.

Table 3. Selected Bond Angles (deg) of $(ap)_4Rh_2(C{\equiv}C)_2Si(CH_3)_3$ (**1**), $(dpf)_4Rh_2(CNC_6H_5)$ (**3**), and $(dpf)_4Rh_2(CNC_6H_4NC)Rh_2(dpf)_4$ (**4**)

$(ap)_4Rh_2(C{\equiv}C)_2Si(CH_3)_3$ (**1**)			
N(1)−Rh(1)−Rh(2)	86.7(1)	N(3)−Rh(1)−Rh(2)	87.0(1)
N(5)−Rh(1)−Rh(2)	86.1(1)	N(7)−Rh(1)−Rh(2)	86.7(1)
N(2)−Rh(2)−Rh(1)	87.4(1)	N(4)−Rh(2)−Rh(1)	86.9(1)
N(6)−Rh(2)−Rh(1)	87.5(1)	N(8)−Rh(2)−Rh(1)	87.4(1)
N(3)−Rh(1)−N(1)	87.3(2)	N(5)−Rh(1)−N(3)	89.0(2)
N(7)−Rh(1)−N(5)	91.8(2)	N(7)−Rh(1)−N(1)	91.1(2)
N(4)−Rh(2)−N(2)	89.5(2)	N(6)−Rh(2)−N(4)	88.6(2)
N(8)−Rh(2)−N(6)	90.6(2)	N(8)−Rh(2)−N(2)	90.7(2)
C(45)−Rh(1)−Rh(2)	179.2(2)	Rh(1)−C(45)−C(46)	178.7(6)
C(45)−Rh(1)−N(1)	94.0(2)	C(45)−Rh(1)−N(3)	93.5(2)
C(45)−Rh(1)−N(5)	93.2(2)	C(45)−Rh(1)−N(7)	92.8(2)
$(dpf)_4Rh_2(CNC_6H_5)$ (**3**)			
N(1)−Rh(1)−Rh(2)	86.09(8)	N(3)−Rh(1)−Rh(2)	85.78(8)
N(5)−Rh(1)−Rh(2)	85.37(8)	N(7)−Rh(1)−Rh(2)	86.71(8)
N(2)−Rh(2)−Rh(1)	87.59(8)	N(4)−Rh(2)−Rh(1)	87.60(8)
N(6)−Rh(2)−Rh(1)	87.89(8)	N(8)−Rh(2)−Rh(1)	87.10(8)
N(3)−Rh(1)−N(1)	90.56(12)	N(5)−Rh(1)−N(3)	90.27(12)
N(7)−Rh(1)−N(5)	88.78(12)	N(7)−Rh(1)−N(1)	89.27(12)
N(4)−Rh(2)−N(2)	90.28(12)	N(6)−Rh(2)−N(4)	89.65(12)
N(8)−Rh(2)−N(6)	89.82(12)	N(8)−Rh(2)−N(2)	89.82(12)
C(53)−Rh(1)−Rh(2)	178.00(9)	Rh(1)−C(53)−N(9)	176.2(3)
C(53)−Rh(1)−N(1)	94.69(12)	C(53)−Rh(1)−N(3)	92.36 (12)
C(53)−Rh(1)−N(5)	93.90(12)	C(53)−Rh(1)−N(7)	95.14 (12)
$(dpf)_4Rh_2(CNC_6H_4NC)Rh_2(dpf)_4$ (**4**)			
N(1)−Rh(1)−Rh(2)	86.3(2)	N(3)−Rh(1)−Rh(2)	85.9(2)
N(5)−Rh(1)−Rh(2)	86.3(2)	N(7)−Rh(1)−Rh(2)	86.3(2)
N(2)−Rh(2)−Rh(1)	87.8(2)	N(4)−Rh(2)−Rh(1)	87.4(2)
N(6)−Rh(2)−Rh(1)	88.4(2)	N(8)−Rh(2)−Rh(1)	87.9(2)
N(3)−Rh(1)−N(1)	90.9(3)	N(5)−Rh(1)−N(3)	89.0(3)
N(7)−Rh(1)−N(5)	89.9(3)	N(7)−Rh(1)−N(1)	89.2(3)
N(4)−Rh(2)−N(2)	89.5(3)	N(6)−Rh(2)−N(4)	89.2(3)
N(8)−Rh(2)−N(6)	90.2(3)	N(8)−Rh(2)−N(2)	90.8(3)
C(53)−Rh(1)−Rh(2)	177.7(2)	Rh(1)−C(53)−N(9)	178.6(8)
C(53)−Rh(1)−N(1)	95.3(3)	C(53)−Rh(1)−N(3)	92.5(3)
C(53)−Rh(1)−N(5)	92.1(4)	C(53)−Rh(1)−N(7)	95.3(3)

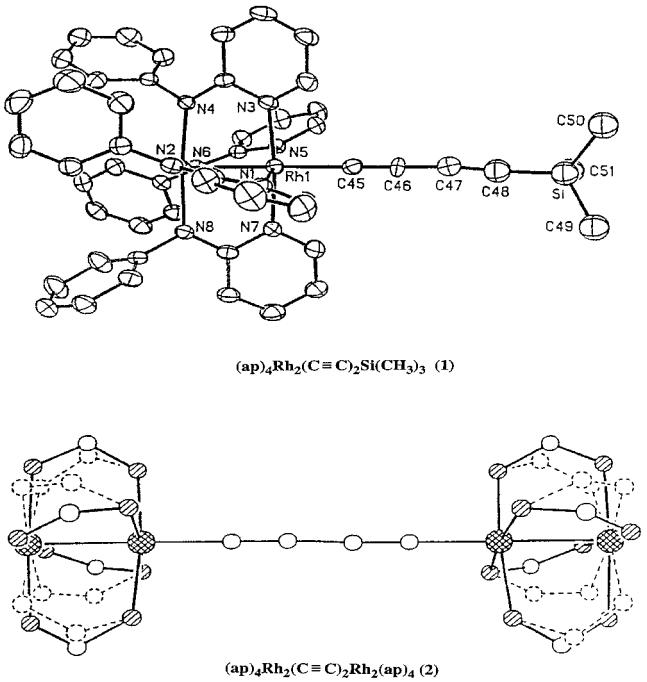

Figure 1. Thermal ellipsoid plot (40% equiprobability envelopes) of $(ap)_4Rh_2(C{\equiv}C)_2Si(CH_3)_3$ (**1**) with ball-and-stick plot of partially solved molecular structure of $(ap)_4Rh_2(C{\equiv}C)_2Rh_2(ap)_4$ (**2**). H atoms have been omitted for clarity.

compounds with respect to their bond geometries. Indeed, the Rh−Rh distance of 2.443(1) Å in **1** is similar to the 2.439(1) Å distance in $(ap)_4Rh_2C{\equiv}CH$.[8] The bond lengths of 1.188(11) Å (see Table 2) and 1.185(3) Å[8] between C45 and C46 in these two complexes are also similar to each other and are within the range of carbon−carbon triple bond lengths of other similar diruthenium or dirhodium complexes.[8,26,31] The heavy disorder of the axial ligand in $(ap)_4Rh_2(C{\equiv}C)_2Si(CH_3)_3$ (**1**) prevented an accurate determination of the C(47)−C(48) bond distance. One structural feature of this compound, which is also seen in compounds **3** and **4**, is that there is a 50:50 mixture of left- and right-handed molecules in the sample crystal with respect to the N−Rh−Rh−N torsion angles, i.e., the crystals are racemic without conformational changes.

Table 4. Half-Wave Potentials in THF or CH_2Cl_2 (V vs SCE)

	oxidation		reduction	
compound	2nd	1st	1st	2nd
$(ap)_4Rh_2(C{\equiv}C)_2Si(CH_3)_3$ (**1**)[a]	none	0.66	−0.44	none
$(ap)_4Rh_2(C{\equiv}C)_2Rh_2(ap)_4$ (**2**)[a]	none	0.60	−0.52	−0.65
$(dpf)_4Rh_2(CNC_6H_5)$ (**3**)[b]	1.22	0.23	none	none
$(dpf)_4Rh_2(CNC_6H_4NC)Rh_2(dpf)_4$ (**4**)[b]	1.20	0.22	none	none

[a] In THF, containing 0.2 M TBAP. [b] In CH_2Cl_2, containing 0.1 M TBAP.

Both $(dpf)_4Rh_2(CNC_6H_5)$ (**3**) and $(dpf)_4Rh_2(CNC_6H_4NC)Rh_2(dpf)_4$ (**4**) contain a Rh_2^{4+} core, and both are bridged by four dpf equatorial ligands with similar axial ligands. The eight Rh−N bond distances of each compound are about the same, averaging 2.06 Å for Rh(1)−N and 2.05 Å for Rh(2)−N in **3** and 2.05 Å for Rh(1)−N and 2.04 Å for Rh(2)−N in **4**. The Rh−Rh bond distances are 2.4798(4) and 2.496(1) Å in **3** and **4**, respectively, and both values are greater than the Rh−Rh distances of 2.457(1) and 2.4599(1) Å in $(dpf)_4Rh_2$ and $(dpf)_4Rh_2(NCCH_3)$,[16] thus suggesting that the CNC_6H_5 axial ligand in $(dpf)_4Rh_2(CNC_6H_5)$ and the CNC_6H_4NC bridging ligand in $(dpf)_4Rh_2(CNC_6H_4NC)Rh_2(dpf)_4$ are both σ-donors and that, in each molecule, they increase the electron density in the antibonding orbitals of the dimetal core.

Each unit in $(dpf)_4Rh_2(CNC_6H_5)$ (**3**) and $(dpf)_4Rh_2(CNC_6H_4NC)Rh_2(dpf)_4$ (**4**) has only 2-fold symmetry about the Rh−Rh axis by virtue of the twist of the phenyl rings, and this was also the case in $(dpf)_4Rh_2$.[16] Apparently, this internal dissymmetry is the driving force behind the orientation of the bridging phenyl ring in **4**. Although the central ring adopts two different orientations, they are only 61° apart, rather than the 90° expected for a unit with 4-fold symmetry. Therefore, there must be some significant steric preference for the observed orientation of the bridging phenyl ring.

Electrochemistry and ESR Characterization. Cyclic voltammograms of the four compounds are shown in Figures 3 and 4, and half-wave potentials of each redox reaction are listed in Table 4. The two ap complexes which contain $Rh_2^{II,III}$ units exhibit processes associated both with reduction to the lower dirhodium(II,II) form and oxidation to the higher dirhodium(III,III) form. This contrasts with the two dpf derivatives each of which contains $Rh_2^{II,II}$ units and exhibits only oxidations to give initially complexes with the dirhodium(II,III) oxidation state and then, at more positive potentials, with diruthenium(III,III) units. No other redox processes are observed within the range of the nonaqueous solvent, i.e., from −1.8 to 1.8 V vs SCE.

The compound $(ap)_4Rh_2(C{\equiv}C)_2Si(CH_3)_3$ (**1**) undergoes a single reversible one-electron oxidation at $E_{1/2} = 0.66$ V and a single reversible one-electron reduction at $E_{1/2} = -0.44$ V in THF, 0.2 M TBAP (Figure 3a). Both processes are reversible and generate a dirhodium(III,III) complex upon oxidation and a dirhodium(II,II) species upon reduction. This result can be

(31) Chakravarty, A. R.; Cotton, F. A. *Inorg. Chim. Acta* **1986**, *113*, 19.

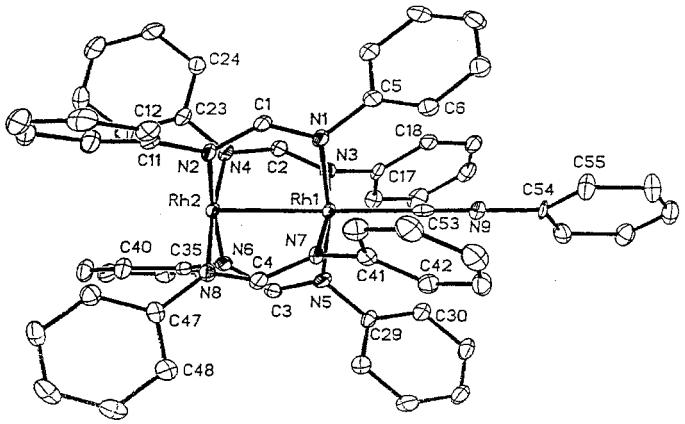

$(dpf)_4Rh_2(CNC_6H_5)$ (**3**)

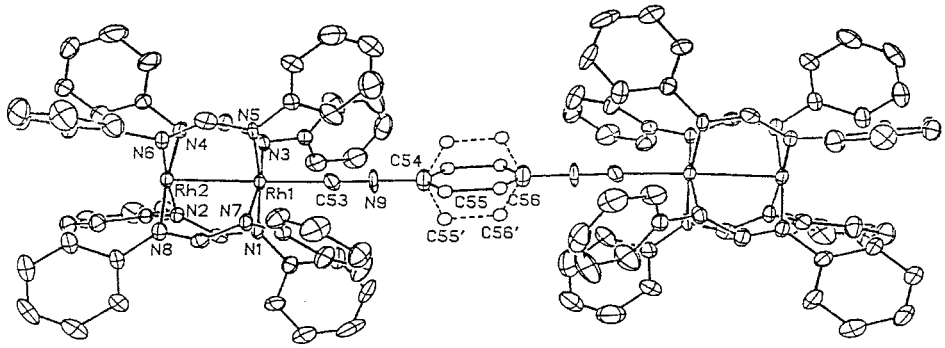

$(dpf)_4Rh_2(CNC_6H_4NC)Rh_2(dpf)_4$ (**4**)

Figure 2. Thermal ellipsoid plot (40% equiprobability envelopes) of $(dpf)_4Rh_2(CNC_6H_5)$ (**3**) and $(dpf)_4Rh_2(CNC_6H_4NC)Rh_2(dpf)_4$ (**4**).

compared with $(ap)_4Rh_2(C{\equiv}C)_2Rh_2(ap)_4$ (**2**), which exhibits a reversible oxidation consisting of two overlapped one-electron transfers at $E_{1/2} = 0.60$ V and two separate reversible one-electron reductions at $E_{1/2} = -0.52$ and -0.65 V (see Figure 3a and Table 4). The overall two-electron oxidation of $(ap)_4Rh_2(C{\equiv}C)_2Rh_2(ap)_4$ (**2**) leads to a bis-dirhodium complex with two Rh_2^{6+} units.

The first reduction of $(ap)_4Rh_2(C{\equiv}C)_2Rh_2(ap)_4$ (**2**) at -0.52 V leads to a bis-dirhodium species containing both Rh_2^{5+} and Rh_2^{4+} cores while the second reduction at -0.65 V leads to a compound which possesses two identical Rh_2^{4+} cores. Normal pulse voltammetry of **2** in THF, 0.2 M TBAP (third curve in Figure 3a), gives a current−voltage curve where the ratio of limiting currents for the oxidations and reductions are in an approximately 2:1:1 ratio, thus further confirming the number of electrons involved in each electrochemical process. The first and second reductions of $(ap)_4Rh_2(C{\equiv}C)_2Rh_2(ap)_4$ (**2**) are separated in potential by 130 mV, thus suggesting electronic interaction between the two dirhodium units. This is not the case upon oxidation of **2**, where two electrons are removed from the compound (one from each $Rh_2^{II,III}$ unit) at the same potential, giving an apparent overlapping two-electron transfer.

The ESR signals of $(ap)_4Rh_2(C{\equiv}C)_2Si(CH_3)_3$ (**1**) and $(ap)_4Rh_2(C{\equiv}C)_2Rh_2(ap)_4$ (**2**) before oxidation or reduction are shown in Figure 3b and exhibit axial symmetry at 77 K in CH_2Cl_2/CH_3CN with $g_\perp = 2.129$ and $g_\parallel = 1.929$ ($A_\parallel = 29 \times 10^{-4}$ cm^{-1}) for **1** and $g_\perp = 2.134$ and $g_\parallel = 1.928$ ($A_\parallel = 43 \times 10^{-4}$ cm^{-1}) for **2**. Similar ESR spectra have been reported for $(ap)_4Rh_2(C{\equiv}CH)$,[8] thus suggesting that compounds **1** and **2** both have the electronic configuration $(\sigma)^2(\pi)^4(\delta)^2(\pi^*)^4(\delta^*)^1$. In both ESR spectra of Figure 3b, the $g_\parallel$ component is split into a doublet, thus indicating that the unpaired electron is localized on one and only one of the two rhodium atoms.[6−8]

Most likely, the Rh(III) ion of each $Rh_2^{II,III}$ unit in $(ap)_4Rh_2(C{\equiv}C)_2Rh_2(ap)_4$ (**2**) is the one bound to the $(C{\equiv}C)_2^{2-}$ group since this axial ligand is a strong σ-donor. The electrochemical data would then suggest that the addition of one electron on the rhodium(III) ion of one dimeric unit in compound **2** is accompanied by a delocalization of electron density over the diacetylide ligand, thus making the second dirhodium unit more difficult to reduce as indicated by the -130 mV shift in $E_{1/2}$ for this reaction.

The cyclic voltammograms of $(dpf)_4Rh_2(CNC_6H_5)$ (**3**) and $(dpf)_4Rh_2(CNC_6H_4NC)Rh_2(dpf)_4$ (**4**) are shown in Figure 4a. Both compounds undergo two reversible oxidations located at $E_{1/2} = 0.23$ and 1.22 V (for **3**) or 0.22 and 1.20 V (for **4**) in CH_2Cl_2, 0.1 M TBAP. The two oxidations of $(dpf)_4Rh_2(CNC_6H_5)$ (**3**) involve well-resolved one-electron-transfer steps, thus implying that the first oxidation of **3** leads to a compound with a Rh_2^{5+} core while the second oxidation generates a complex with a Rh_2^{6+} core.

The overall two-electron oxidation of $(dpf)_4Rh_2(CNC_6H_4NC)Rh_2(dpf)_4$ (**4**) occurs at an $E_{1/2}$ value almost identical to the halfwave potential for oxidation of **3** (see Table 4). Bulk controlled-potential coulometry confirms that two electrons are removed from compound **4** during the first oxidation and a similar number of electrons abstracted is proposed for the second oxidation since the first and second oxidation processes have similar peak current heights (Figure 4). The fact that each oxidation of compound **4** involves two overlapped one-electron-transfer processes suggests that there is little electronic communication between the two dirhodium units in either the neutral

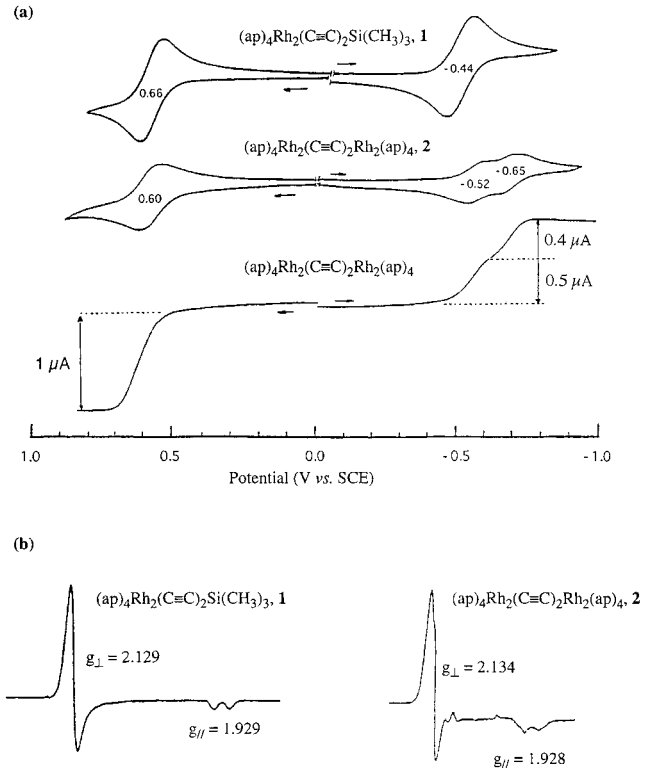

Figure 3. (a) Cyclic voltammograms of $(ap)_4Rh_2(C{\equiv}C)_2Si(CH_3)_3$ and $(ap)_4Rh_2(C{\equiv}C)_2Rh_2(ap)_4$ as well as a normal pulse voltammogram of $(ap)_4Rh_2(C{\equiv}C)_2Rh_2(ap)_4$ in THF, 0.2 M TBAP. (b) ESR spectra of $(ap)_4Rh_2(C{\equiv}C)_2Si(CH_3)_3$ and $(ap)_4Rh_2(C{\equiv}C)_2Rh_2(ap)_4$ in CH_2Cl_2/CH_3CN at 77 K.

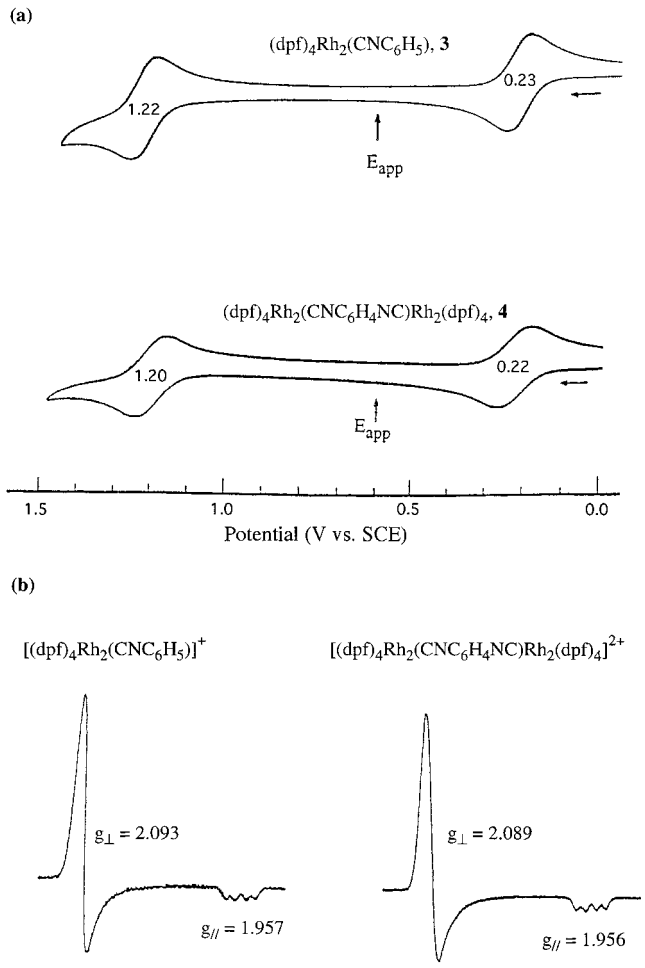

Figure 4. (a) Cyclic voltammograms of $(dpf)_4Rh_2(CNC_6H_5)$ and $(dpf)_4Rh_2(CNC_6H_4NC)Rh_2(dpf)_4$ in CH_2Cl_2, 0.1 M TBAP. (b) ESR spectra of $[(dpf)_4Rh_2CNC_6H_5]^+$ and $[(dpf)_4Rh_2(CNC_6H_4NC)Rh_2(dpf)_4]^{2+}$ at 77 K in CH_2Cl_2, 0.1 M TBAP.

or oxidized forms of $(dpf)_4Rh_2(CNC_6H_4NC)Rh_2(dpf)_4$. Compound **4** is thus converted to a bis-dirhodium complex with two non-interacting Rh_2^{5+} cores after the first two-electron oxidation and a compound with two Rh_2^{6+} cores after the second two-electron oxidation.

No reduction of $(dpf)_4Rh_2(CNC_6H_5)$ (**3**) or $(dpf)_4Rh_2(CNC_6H_4NC)Rh_2(dpf)_4$ (**4**) is observed within the negative potential limit of the solvent (~ -1.8 V), and this contrasts with $Rh_2(dpf)_4$, where a single reduction of the compound is observed at $E_{1/2} = -1.21$ V under the same solution conditions.[16] This result suggests that the LUMOs of $(dpf)_4Rh_2(CNC_6H_5)$ (**3**) and $(dpf)_4Rh_2(CNC_6H_4NC)Rh_2(dpf)_4$ (**4**) have higher energy than the LUMO of $Rh_2(dpf)_4$, and this can be accounted for by the increased electron density in the antibonding orbitals of the dimetal core, due to the σ-donor properties of the CNC_6H_5 and CNC_6H_4NC axial ligands. This result also agrees with the fact that the Rh−Rh bond distances of **3** and **4** are both larger than the Rh−Rh bond distance of $Rh_2(dpf)_4$.

The compounds $(dpf)_4Rh_2(CNC_6H_5)$ (**3**) and $(dpf)_4Rh_2(CNC_6H_4NC)Rh_2(dpf)_4$ (**4**) are both ESR silent in their neutral form, but the first oxidation products of **3** and **4** generated by controlled-potential bulk electrolysis in CH_2Cl_2, 0.1 M TBAP, at 0.60 V under an Ar atmosphere are both ESR active (see Figure 4b). The ESR signals of the compounds have axial symmetry at 77 K with $g_\perp = 2.093$ and $g_{||} = 1.957$ ($A_{||} = 11 \times 10^{-4}$ cm^{-1}) for $[\mathbf{3}]^+$ or $g_\perp = 2.089$ and $g_{||} = 1.956$ ($A_{||} = 12 \times 10^{-4}$ cm^{-1}) for $[\mathbf{4}]^{2+}$. Each $g_{||}$ component is split into a doublet of doublets, thus indicating that the unpaired electron in both compounds has an unequal distribution of spin density in the dirhodium unit.[16,32] Therefore, the oxidized form of $(dpf)_4Rh_2(CNC_6H_4NC)Rh_2(dpf)_4$ (**4**) can be described as a bis-dirhodium complex with two independent Rh_2^{5+} cores, each of which has unpaired spin density unequally distributed over the two rhodium ions. This is similar to the electronic distribution in $(ap)_4Rh_2(C{\equiv}C)_2Rh_2(ap)_4$ (**2**), except that in **2** the unpaired spin density is localized on only one rhodium atom of each dirhodium unit.

Acknowledgment. The support of the Robert A. Welch Foundation (J.L.B., Grant E-918; K.M.K., Grant E-680) is gratefully acknowledged. We thank Dr. J. K. Korp for performing the X-ray analyses for compounds **1**, **2**, and **4** and Dr. Douglas Powell for X-ray analysis of compound **3**. B.H. also acknowledges Mr. S. Erickson for preliminary experiments involving compound **3**. Funds from NSF Grant CHE-9310428 and from the University of Wisconsin were used to purchase the X-ray instruments and computers used in the determination of **3**.

Supporting Information Available: Tables of data collection parameters, atomic coordinates, anisotropic displacement parameters, and all molecular bond lengths and angles and views of the molecules as well as molecular packing diagrams. This material is available free of charge via the Internet at http://pubs.acs.org.

IC001245F

(32) Le, J. C.; Chavan, M. Y.; Chau, L. K.; Bear, J. L.; Kadish, K. M. *J. Am. Chem. Soc.* **1985**, *107*, 7195.